JVI Accepted Manuscript Posted Online 26 February 2020
J. Virol. doi:10.1128/JVI.01918-19

Identification and cloning of a new western Epstein-Barr virus strain that replicates efficiently in primary B cells

Susanne Delecluse[1,2,3,4], Remy Poirey[1,2,3], Martin Zeier[4], Paul Schnitzler[5], Uta Behrends[3,6,7], Ming-Han Tsai[8]*, Henri-Jacques Delecluse[1,2,3]*

[1]German Cancer Research Centre (DKFZ) Unit F100, Heidelberg, Germany

[2]Institut National de la Santé et de la Recherche Médicale (INSERM) Unit U1074, Heidelberg, Germany

[3]German Center for Infection Research (DZIF)

[4]Nierenzentrum Heidelberg, Heidelberg, Germany

[5]Center for Infectious Diseases, Virology, University Hospital Heidelberg, Heidelberg, Germany

[6]Children's Hospital Schwabing, Technische Universität München, Munich, Germany

[7]Research Unit Gene Vectors, Helmholtz Zentrum München, German Research Center for Environmental Health, Munich, Germany

[8]Institute of Microbiology and Immunology, National Yang-Ming University, Taipei, Taiwan

*Corresponding authors

Correspondence:

Ming-Han Tsai (m.tsai@ym.edu.tw)

Henri-Jacques Delecluse, (h.delecluse@dkfz.de)

Running title: EBV replication in B cells

Abstract

The Epstein-Barr virus (EBV) causes human cancers and epidemiological studies have shown that lytic replication is a risk factor for some of these tumors. This fits with the observation that EBV M81 that was isolated in a Chinese patient with nasopharyngeal carcinoma induces potent virus production and increases the risk of genetic instability in infected B cells. To find out whether this property extends to viruses found in other parts of the world, we investigated 22 viruses isolated from Western patients. While one third of the viruses hardly replicated, the remaining ones showed variable levels of replication with three isolates replicating at levels close to M81 in B-cells. We cloned one strongly replicating virus into a bacterial artificial chromosome; the resulting recombinant virus (MSHJ) retained the properties of its non-recombinant counterpart and showed similarities with M81, undergoing lytic replication *in vitro* and *in vivo* after three weeks of latency. In contrast, B-cells infected with the non-replicating western B95-8 virus showed an early but abortive replication accompanied by cytoplasmic BZLF1 expression. Sequencing confirmed that rMSHJ is a western virus, being genetically much closer to B95-8 than to M81. Spontaneous replication in rM81- and rMSHJ-infected B-cells was dependent on phosphorylated Btk and was inhibited by exposure to ibrutinib, opening the way to clinical intervention in patients with abnormal EBV replication. As rMSHJ contains the complete EBV genome and induces lytic replication in infected B-cells, it is ideal to perform genetic analyses of all viral functions in western strains and their associated diseases.

Importance

The Epstein-Barr virus (EBV) infects the majority of the world population but causes different diseases in different countries. Evidence that lytic replication, the process that leads to new virus progeny, is linked to cancer development is accumulating. Indeed, viruses such as M81 that were isolated from Far East nasopharyngeal carcinomas replicate strongly in B-cells. We now show that some viruses isolated from western patients, including the MSHJ strain share this property. Moreover, replication of both M81 and of MSHJ was sensitive to ibrutinib, a commonly used drug, thereby opening an opportunity for therapeutic intervention. Sequencing of MSHJ showed that this virus is quite distant from M81 and much closer to non-replicating western viruses. We conclude that western EBV strains are heterogeneous, some viruses being able to replicate stronger and therefore being potentially more pathogenic than others, and that the virus sequence information alone cannot predict this property.

Introduction

The Epstein-Barr virus (EBV) is a member of the gammaherpesvirinae family that causes infectious mononucleosis (IM) and malignant diseases (1). EBV is strongly B-lymphotropic and etiologically associated with B cell lymphoproliferations whose incidence rises strikingly in immunosuppressed individuals (1). This population includes elderly patients and patients with acquired immune deficiency, e.g. after HIV infection or intake of immunosuppressive drugs in solid organ (SOT) or stem cell transplantation (SCT) recipients (2). The latter patients develop posttransplant lymphoproliferative disorders (PTLD) that frequently express the EBV latent genes, as well as EBV microRNAs (1, 3).

In infected B-cells, EBV classically induces a viral latency that is characterized by cell proliferation, expression of the full set of latent genes and absent or limited lytic replication, the process that leads to the production of virus progenies (1). These characteristics are easily identifiable in B-cells infected with the B95-8 strain either *in vitro* or in infected humanized mice (4). B95-8 was isolated from a US patient with infectious mononucleosis and is thought to be representative of the virus found in IM patients, and more generally in the western population. However, we have recently shown that the M81 virus isolated from a Chinese patient with nasopharyngeal carcinoma (NPC), induces potent lytic replication in B-cells from normal individuals, both *in vitro* and in humanized mice (4).

Epidemiological studies have identified virus lytic replication as a risk factor for the development of some EBV-associated lymphomas and carcinomas (5). High antibody titers against EBV replicative antigens are predictive of NPC several years in advance (6). Furthermore, more than 90% of EBV-positive PTLD contain cells undergoing replication and express BZLF1, the key viral transactivator that initiates EBV lytic

replication, or early and late EBV lytic antigens such as EA-D (7). Similar features were recorded in AIDS-associated lymphomas (8). We recently demonstrated that the EBV particles themselves can confer chromosomal instability and aneuploidy after contact with target B-cells (9). This establishes a direct mechanistic link between lytic replication and cancer risk development.

In this paper, we report the properties of viruses present in spontaneous cell lines generated from 13 transplant recipients, and from 9 patients with IM. We cloned the genome of one of these viruses that displayed potent replication in primary B-cells onto a bacterial artificial chromosome (BAC) and compared its characteristics to those of well-characterized laboratory strains.

Results

Spontaneously-growing EBV-transformed B-cells from patients with IM or iEBVL frequently replicate the virus, although with greatly varying intensity.

We first generated a panel of spontaneously growing EBV-transformed lymphoblastoid cell lines (LCL) from patients with IM or with an increased EBV load in the peripheral blood (>1000 cop/ml) (iEBVL) (Table 1). These were established very easily from most patients within less than four weeks from approximately 10E5 peripheral blood B-cells. We stained them shortly after establishment with antibodies specific to BZLF1 and gp350 to assess lytic replication (Fig. 1). Four weeks after seeding, 12 from 13 EBVL and 7 from 9 IM cell lines expressed the immediate early (IE) lytic protein BZLF1 and the late protein gp350 (Fig. 1). Thus, only one of the iEBVL (sLCL-10) and two of the IM cell lines (IM-7 and IM-8) were devoid of any lytic protein expression. Two thirds of the cases contained more than 1% BZLF1 positive cells, seven cases between 2 and 5.7% of BZLF1-positive cells, four of which showed replication levels close to those reached by M81. However, only five EBVL and five IM cell lines expressed the late lytic protein gp350 in more than 1% of cells and only one case reached M81 levels, in terms of combined BZLF1 and gp350 expression (Fig. 1). Here we took into consideration only cells expressing gp350 in the entire cytoplasm and excluded cells showing patchy gp350-specific staining at the cell surface that we interpreted as B-cells partially covered with bound viruses (Fig. 1). Whilst the EBV genome adopts a circular conformation in latently infected B-cells, EBV lytic replication results in the generation of linear genomes (1). We assessed the structure of the EBV genomes present in our panel of LCLs using Gardella gel analyses. These assays revealed the presence of linear genomes in cell lines that were found to produce lytic proteins, thereby confirming that these cells supported lytic replication (Fig. 2A). We examined four cell lines that

showed signs of lytic replication in electron microscopy and could confirm the presence of mature virions in the infected cell population (Fig. 2B). Interestingly, we frequently found viruses bound at the B cell surface confirming the results of the gp350-specific staining. This was expected as these cells express the EBV receptor CD21. We then attempted to infect and immortalize primary B-cells with supernatant from our LCL panel. Although many viruses were bound to the cell surface, this experiment nevertheless succeeded in 5/9 IM sLCLs and in 8/13 iEBVL sLCLs (Fig. 3A and B). When daughter cell lines could be established from these supernatants, they exhibited the characteristics of the cell line from which the viruses were produced in terms of gp350 and BZLF1 expression, demonstrating that the properties observed in the initial cell lines reflected the intrinsic properties of the virus (Fig. 3A and B). We then monitored the ability of the sLCLs to support lytic replication over time. Three months after establishment of the LCLs, gp350 expression decreased but remained detectable in 4 iEBVL (2 comparable to M81, 2 weaker than M81) and in 3 IM B cell lines (3 weaker than M81) (Fig. 2C). We have previously reported a correlation between the growing characteristics of our sLCL panel and their miRNA expression profile (10). This gave us an opportunity to assess the relation between miRNA expression and lytic replication. However, we could only identify a weak correlation between miR-BHRF1-3 expression levels and the ability to support lytic replication (Pearson coefficient r=0.4836, p=0.049).

Most iEBVL and IM strains are genetically related to B95-8.

We wished to identify that molecular events that govern the variable replication rates observed across the investigated panel and first turned our attention to the BZLF1 promoter. Indeed, the BZLF1 promoter contains multiple binding site for transcription

factors and is considered to be a crucial regulatory element for the cell's decision to produce the BZLF1 protein (11). LCLs infected with M81 express lytic proteins at high level, and this phenotype has indeed been ascribed to some extent to polymorphisms in the BZLF1 gene of this virus (4). Therefore, we cloned and sequenced the BZLF1 promoter, its introns and its open reading frame from our virus panel (Table 2). We found that the sequence of all BZLF1 alleles was very close to those of western viruses isolated from patients with IM or PTLD, and in particular lacked the Zp-V3 polymorphism that is commonly found in viruses endemic in East Asia and that was recently shown to confer high replication abilities (12) (13). We noticed that viruses sharing the same BZLF1 sequence showed a highly variable propensity to replicate (compare sLCL-2 and sLCL-5 or IM-6 and IM-7, see Fig.1), demonstrating first that the Zp-V3 polymorphism is not a prerequisite for potent and sustained spontaneous lytic replication and second that the sequence of the BZLF1 gene is not the only parameter that governs this process. Sequencing of the EBNA2 gene showed that all viruses were of type 1 (Table 2). These data confirmed that EBV strains very close to B95-8 are dominant in Western countries.

EBV replication in LCLs is poorly sensitive to inducers.

LCLs are classically refractory to lytic replication and multiple chemical inducers have been used to increase virus production in these cells. Therefore, we investigated the sensitivity of sLCLs that had been in culture for 90 days to these molecules. We treated cells with TPA combined to butyrate, ionomycin and TGF beta. None of these substances induced lytic replication in non-permissive sLCLs. However, when we exposed the sLCLs that supported lytic replication to TPA combined to butyrate or to TGF beta, these substances increased replication of the cell lines on average by 60 and

50%, respectively, although there was a large variation in the amplitude of the effect in the individual viruses (Fig. 3C). Ionomycin had, on average, hardly any effect on the replication of the sLCL panel (average x 1.2 increase) (Fig. 3C). Some cell lines were more sensitive to the drug, although their absolute level of replication remained low.

Cloning of a new EBV western strain on a BAC.

To be able to accurately study the properties of a virus endowed with a high lytic replication rate, we both infected marmoset B-cells with the sLCL-2 virus and cloned its genome onto a BAC replicon. We choose this line because it maintained high levels of gp350 over time and upon passaging to fresh B cells. The resulting marmoset cell line displayed high levels of spontaneous replication and produced infectious virus in the supernatant that is easy to harvest (Fig. 4A). To clone sLCL-2, a BACmid flanked by sequences specific to the EBV terminal repeats was introduced into marmoset B-cells infected by sLCL-2 and subjected to hygromycin selection. The recombinant viral genome, dubbed rMSHJ, was rescued from hygromycin-resistant cells and introduced into *E.coli* cells in which it was subjected to restriction analysis and sequencing (Fig. 4B). This assay showed that the restriction pattern of this recombinant virus differs from the one generated by digestion of the recombinant M81 and B95-8 genomes. The rMSHJ has four terminal repeats before the BACmid and three after it. Complete sequencing of the rMSHJ genome allowed alignment to previously available viral sequences and the construction of a genetic tree (Fig. 5). In parallel, we sequenced the complete genome of the replicating IM-3 cell line to obtain a second viral sequence. Both genomes clustered with western strains, and in particular B95-8, but were distinct from it (Fig. 5). We found 654 non-synonymous mutations in rMSHJ relative to B95-8, i.e. in approximately 0.48% of the genome, and 524 in IM-3 relative to B95-8, i.e. in

approximately 0.39% of the genome (Table 3). Interestingly, both viruses were closer to each other (280 mutations) than to B95-8 (Table 3). The mutations in both IM-3 and rMSHJ were homogeneously distributed across the genome (Tables 4 and 5). However, as previously noted, viral latent genes displayed on average more non-synonymous mutations than lytic genes (14). Among latent genes, EBNA1, EBNA2, LMP1 and LMP2 were the most polymorphic (Tables 4 and 5).

Phenotypic characteristics of rMSHJ.

Stable introduction of the rMSHJ genome into 293 cells allowed efficient virus production and thus a detailed characterization of the virus properties. Viral titers upon induction were in the range of 5x10E7 genome equivalents per ml, as defined by qPCR, and thus intermediate between rB95-8 (1x10E7/ml) and rM81 (1x10E8/ml). We began the characterization of rMSHJ by infecting primary B-cells. Exposure of B-cells to rMSHJ, rM81 and rB95-8 led to primary B-cells infection, but the infection efficiency was nearly five times higher with rB95-8 than with rMSHJ or rM81 as determined by EBNA2 staining, a viral protein expressed shortly after infection (Fig. 6A). We then performed transformation assays in 96-well cluster plates coated with feeder cells. These assays showed that seeding of 3 EBNA2-positive B-cells after infection with rMSHJ and rM81, led to a similar number of transformed colonies. However, this number was two to three times lower than after infection with rB95-8. Thus, rB95-8 is more transforming than rMSHJ or rM81 (Fig. 6B). We complemented this approach by comparing the growth rate of LCLs freshly established with the different viruses. These assays showed that B95-8-infected B-cells grew more quickly than after infection with rMSHJ, with B-cells transformed by rM81 being the slowest (Fig. 6C). B-cells transformed by these viruses showed expression of latent genes, although some

variations in the expression level and size of the proteins was noted as previously described (15) (data not shown). Some of these differences can result from the polymorphisms identified in the latent genes that lead to a variable affinity of the antibodies for the viral proteins. We then performed infections on primary epithelial cells derived from the respiratory epithelium that covers the sphenoidal sinus with rMSHJ, rB95-8 or rM81 and stained infected cells for EBER expression (Fig. 7A and B) (16). We performed direct infections or transfer infections using primary B-cells coated with viruses (17). These assays showed that rMSHJ can infect epithelial cells, but with lower efficiency, 5 to 50%, relative to rM81. As previously reported, B95-8 could not infect these cells (4). We then monitored the ability of B-cells infected with this virus panel to initiate and complete lytic replication. To this end, we stained B-cells at weekly intervals with antibodies specific to BZLF1 and gp350 (Fig. 8A). This analysis revealed that the B cell populations infected with rB95-8 showed some BZLF1-positive cells one-week post-infection, although signals were weak and mainly located in the cytoplasm of infected cells and very rarely in the nucleus. These cells did not express gp350. This pattern remained visible for the following weeks with a regular decrease in the number of BZLF1-positive cells across the four weeks of observation. B-cells infected with rM81 and rMSHJ showed a different pattern of expression. While in both cases BZLF1 signals could be detected in the cytoplasm after one week of infection, cells showing BZLF1-specific nuclear signals became visible only in the third week post infection. At this time point, a minority of infected cells were strongly gp350-positive, and the majority of cells showed viruses bound to their surface. However, the percentage of gp350-positive cells was clearly higher in cells infected with rM81 than in those infected with rMSHJ. This pattern remained similar for another 3 weeks, with a steady increase in the number of replicating cells. At six weeks post-

infection, the number of B-cells infected with rM81 that produced BZLF1 was on average higher than their counterparts infected with rMSHJ, and the difference was even more pronounced for gp350 (Fig. 8B). A western blot analysis confirmed expression of these lytic proteins after infection with rM81 and rMSHJ1, although infection with the former led to stronger Fgp350 expression (Fig. 8C). This assay also showed that the BZLF1 protein produced by cells infected with rMSHJ has a lower molecular weight than the species produced by cells infected with rM81. This difference was previously noted after transfection of the B95-8 BZLF1 gene (4).

B cells infected with rMSHJ replicate in an *in vivo* murine model

We wished to confirm some of our data in an *in vivo* animal model. Therefore, we injected primary B-cells coated with rMSHJ or rM81 into immunosuppressed NSG-A2 mice (18). 5 weeks after injection, mice developed tumors. Immunohistological stains revealed that for both viruses, these tumors expressed both BZLF1 and gp350 (Fig. 8D). We found that 8.7% of EBER-positive cells underwent replication 5 weeks post infection as assessed by BZLF1 expression after infection with rMSHJ that compares with 7.2% after infection with rM81. Thus, there is a good correlation between the *in vitro* and the *in vivo* data, although tumors *in vivo* could only be analyzed at a single time point (5 weeks post infection). Injection of the IM-3 cell line revealed a similar pattern, although gp350 was less strongly expressed (data not shown).

B-cells infected by rM81 or rMSHJ are responsive to a Btk-specific inhibitor.

The role of the B cell receptor signaling complex on EBV lytic replication has been well established and we wished to study its impact on spontaneously replicating EBV-infected B cells. To this end, we transformed a set of three independent B cell samples

with rB95-8, rM81 or rMSHJ and exposed them to ionomycin or to immunoglobulins directed against the B cell receptor to activate calcium-dependent pathways. While the latter treatment had no statistically significant effect on the replication rate of any of the different types of infected cells, the former potentiated it only in one cell sample infected by rM81 (Fig. 3D). We then blocked calcium signaling in these cells by exposing them to cyclosporin A. This treatment led to an average 30% reduction in the number of BZLF1-positive B-cells infected by rM81 that did not reach statistical significance, but had no effect in B-cells infected with rB95-8 or rMSHJ (Fig. 3D). We extended our investigations to modulators of the proximal arm of the BCR cascade by treating our panel of cell lines with Ibrutinib at concentrations known to inhibit Btk only (10 nM) (19). This led to a clear reduction of lytic replication in B-cells infected with rM81 and with rMSHJ, although the effects were less pronounced in the latter case (Fig. 9A). As expected, the treatment with ibrutinib led to a reduction in the amount of p-Btk and of p-Akt-1 in treated LCLs, one of its downstream targets (Fig. 9B). All tested LCLs expressed p-Btk, irrespective of their ability to support lytic replication (Fig. 9B). Increase of Ibrutinib to 100nM completely inhibited replication. Importantly, exposure to Ibrutinib at both concentrations did not affect cell viability or cell growth (Fig. 9C, 9D). Similar though less pronounced effects were observed in B-cells infected by rMSHJ. Finally, we exposed infected cells to the mTORC1 inhibitor Rapamycin that was previously reported to inhibit induced lytic replication (20, 21). This treatment indeed nearly completely blocked BZLF1 expression in both B-cells transformed by rMSHJ and in B-cells transformed by rM81, but it substantially decreased cell viability and division (Fig. 9A, 9C, 9D).

Infected B-cells that have lost permissivity to spontaneous EBV replication can be rescued by hypoxia treatment.

Previous reports have shown that iron chelators that mimic hypoxia potentiate lytic replication in infected BL cells (22). We wished to test whether hypoxia also modulated spontaneous lytic replication in infected B-cells. To this end, we grew B-cells that had been infected with rB95-8, rM81 and rMSHJ for 30 days in a hypoxic chamber (1% oxygen) for up to one week and monitored BZLF1 protein expression in these cells. This treatment had no effect on B-cells infected with rM81 or rMSHJ (Fig. 10A). However, we observed the appearance of nuclear BZLF1 signals in cells infected with rB95-8, although the percentage of positive B-cells remained between 0.07 and 0.6%. We repeated this experiment with LCLs that had been in culture for more than three months and whose replication rates were reduced by 80%, relative to their peak. Hypoxia led to a 3 to 4-fold increase in the number of BZLF1-positive B-cells infected by rMSHJ or rM81 and again to the appearance of a few B95-8-transformed B cells with genuine BZLF1-positive nuclear signals (<0.5%) (Fig. 10A). Western blot also showed upregulation of BZLF1 and gp350 after infection with rM81 and rMSHJ (Fig. 10A). We also observed a parallel decrease in LMP1 expression as the result of hypoxia treatment, associated to a reduction in EBNA2's molecular weight. These changes correlated with an increase in apoptosis, as assessed by the appearance of cleaved PARP. We then investigated tumors induced by rM81 and rMSHJ infection in immunosuppressed mice to study the relationship between vascularization and lytic replication. Previous work had found that replicating cells were located at distance from vessels, suggesting that it was facilitated by a more hypoxic environment (22). This approach used an experimental system that visualizes larger vessels but not microvessels or capillaries. However, tissue oxygenation mainly depends on

microvessels that are too small to be visible with this method (23). Therefore, we stained tissues for both BZLF1 and CD34, a marker of endothelial cells (24). This approach showed that all BZLF1-positive B-cells are located in direct vicinity of capillaries (Fig. 10B), although the distance of these cells to large arteries varied more widely, ranging from 20 to 650 micrometers, with a mean distance of 400 micrometers (Fig. 10C). Therefore, we can confirm that replicating B-cells are enriched at a certain distance from larger blood vessels, but this does not translate into a significant distance from capillaries.

Discussion

EBV infects primary B-cells and epithelial cells, but the outcome of infection is classically different in these two types of cells. While infected B-cells initiate unlimited cell growth, epithelial cells support lytic replication (1). This dichotomy is based on early investigations that showed that infection of primary B-cells with the prototypical B95-8 strain does not lead to any measurable virus production, although the cellular background also modulates this property (25, 26). Similarly, early reports showed that spontaneously growing LCLs from individuals with IM did not produce any virus (27). However, approximately half of solid organ or bone marrow transplant recipients carry B-cells that showed some signs of lytic replication, for example presence of BZLF1 or gp350 transcripts or of linear DNA, suggesting that they are infected by particular strains or that the clinical context markedly modifies the balance between the virus and its host (28-32). Similarly, spontaneously growing LCLs from healthy individuals or from patients with rheumatoid arthritis displayed variable level of VCA production that, however, never exceeded 1% of the infected cells (27). Interestingly, B-cells infected by type 2 viruses produced viral capsid antigen in western blot at much higher levels than those infected with their type 1 counterparts (33). We now show that most samples of a panel of western type 1 viruses showed evidence of some degree of lytic replication coupled in many cases to spontaneous virus production that was visible in electron microscopy and allowed passaging of the virus to uninfected B-cells, a property that was not investigated in most previous studies. These daughter cell lines retained the ability to produce viruses, suggesting that this property is largely virus-specific. Some transformed B cell samples were exclusively latently infected and could not been induced to produce virus after treatment with TPA and butyrate. Because these viruses cannot be passaged to other B-cells, we cannot formally exclude that they might have

replicated in B-cells from other individuals. Altogether, these data confirm earlier studies that many type 1 EBV-transformed B-cells express low levels of lytic proteins for a limited period of time with an essentially abortive profile characterized by a gp350 expression in up to 1% of the cells. However, they also show that 3 out of 22 of western type 1 viruses induce an unusually potent and sustained lytic replication in infected B-cells. The identification of potent lytic replication in B-cells from transplant recipients or IM patients suggests that these cells are at an increased risk of genetic instability (9). In this line, it is important to note that a large subset of PTLD carry genetic abnormalities (34).

A strict comparison between our strongly replicating EBV isolates and M81 is not meaningful as they infected different cells, had been growing for a variable length of time and also because the antibodies used in immunostains recognize lytic proteins with variable affinity owing to polymorphisms. However, infection of the same B cells with rM81 and rMSHJ showed that the rM81 replication rate remains clearly higher *in vitro*. Inducers of lytic replication such as TPA, ionomycin, TGF-beta or modulators of the B cell receptor generally only weakly enhanced the replication rate. This suggests that the pathways successfully activated by these drugs in other EBV replication cellular systems have comparatively little influence on infected primary B-cells permissive to spontaneous replication.

Cloning and study of rMSHJ revealed differences between EBV strains. In contrast to rB95-8 that induces a transitory lytic protein expression within one week after infection, rM81 and rMSHJ infection led to sustained lytic protein expression that began only at three weeks post-infection, as previously described for rM81 (4). This suggests that multiple events must take place in the infected cell before replication can start, one of which being presumably DNA methylation of the viral genome. Indeed,

BZLF1 preferentially binds to methylated DNA (35). A second difference was that while replicating cells infected by rM81 and rMSHJ mainly showed nuclear BZLF1 expression with a few cells showing cytoplasmic signals, cells infected by rB95-8 mainly displayed BZLF1-specific cytoplasmic signals. This suggests the existence of a mechanism that regulates the location of the protein within different cell compartments. Finally, B-cells infected by rMSHJ and rM81, but not rB95-8, produced late proteins such as gp350 but also infectious virus, suggesting that polymorphisms in the B95-8 genome cells both reduce initiation and completion of the lytic cycle.

Sequencing of rMSHJ and of IM-3 confirmed the close proximity with B95-8, although they differed by 654 and 524 nt, respectively. The polymorphisms were distributed across the genome and it remains unclear at this stage which of these explain the various ability of these viruses to replicate (S1 Table). Sequencing the BZLF1 open reading frame and miniZp promoter thereof in our complete virus panel revealed that all of them are within the western group and 21/22 viruses are within the B95-8 subgroup and lack the Zp-V3 polymorphism. This fits with previous reports showing that patients with IM carry viruses that are very closely related to B95-8 (36). However, the replicating abilities of these strains widely varied, suggesting that polymorphisms outside of BZLF1 modulate this property. Other genetic elements such as EBER2 have been found to modulate the ability of some viral strains to support spontaneous lytic replication (37). We conclude that although some western viruses are genetically close to B95-8, they are sufficiently polymorphic to display variable properties. Which viral genes govern spontaneous lytic replication in B-cells infected with rMSHJ will be revealed by the analysis of the polymorphisms between rM81, rMSHJ and rB95-8. RM81-infected B-cells showed an inconstant and weak sensitivity to modulation of the

B cell receptor pathway through treatment with cyclosporine A, or Ionomycin. B-cells infected by rMSHJ or rB95-8 were even less sensitive to these treatments.

In contrast, Btk was required for a potent spontaneous lytic replication both after infection with rMSHJ and rM81 (Fig. 9A). This inhibitor reduced the levels of p-Btk and its downstream pAkt-1 in treated cells (Fig. 9B). This treatment did not affect cell viability or cell growth (Fig. 9C and D). Treatment of induced BL cells with ibrutunib was previously reported to prevent lytic replication, although the doses used in this study were much higher and probably inhibited other kinases and cell viability (Fig. 9C and D) (20). As Ibrutinib has been extensively used in the treatment of lymphomas at doses similar to those used in this study, this drug might show therapeutic properties in EBV-associated diseases in which lytic replication is high such as chronic EBV infection or even some cases of PTLD. Rapamycin has similar properties, suggesting that mTORC1 is important for all types of EBV lytic replication, although it is unclear which of the multiple targets of this kinase are important for this process (20, 21). We could confirm that hypoxia activates spontaneous lytic replication of both rM81 and rMSHJ, but only in cells that had lost permissivity after several months in culture. In contrast, hypoxia had no effect on spontaneous lytic replication at its peak, one-month post-infection. Similarly, analysis of tissues infected by rMSHJ and rM81 showed that efficient replication in cells located very close to capillaries, confirming that hypoxia is not strictly necessary for spontaneous replication.

In conclusion, we have identified strongly replicating type 1 western viruses that are closely related to B95-8, do not display the Zp-V3 polymorphism and are sensitive to ibrutinib. In contrast to rB95-8, rMSHJ will allow the genetic analysis of all EBV viral functions.

Materials and Methods

Spontaneous cell lines

Thirteen spontaneously growing LCLs were established from B-cells of thirteen immunosuppressed patients with increased EBV load (iEBVL) (sLCL-2 to -15, there is no sLCL-13) and nine sLCLs were generated form the B-cells of nine immunocompetent patients suffering from IM (IM-1 to -10, there is no IM-5). An iEBVL was defined by >1000 cop/ml, as determined by qPCR of a whole blood sample. The ethics committee of the University of Heidelberg approved the study (approval S/005-2014). Patients suffering from IM were diagnosed in Munich by the detection of EBV-specific IgM antibodies and were recruited to the IMMUC study (approval 112/14). 1x10E5 B-cells from the blood of patients with IM or iEBVL were purified and seeded onto NHDF feeder cells. These peripheral blood $CD19^{+}$ B-cells were isolated by ficoll density gradient followed by selection with anti-CD19 PanB Dynabeads and detachment of the beads (Invitrogen). Control cell lines included LCLs generated with rM81 and rB95-8, as well as the Burkitt's cell lines Raji and Elijah (EBV-negative clone thereof). The M81 virus was isolated from a Hong Kong NPC cell line (38). B95-8 was isolated from a US patient with infectious mononucleosis (39). Raji is an EBV-positive BL cell line (40). The rMSHJ cell line was generated by infection of common marmoset peripheral B-cells with the EBV sLCL-2 virus that was isolated from a German stem cell transplant recipient with iEBVL (Table 1).

BAC cloning

A pMBO131-based plasmid carrying a prokaryotic F-factor origin of replication, the chloramphenicol (cam) resistance marker for prokaryotic selection, a SV40 promoter-driven hygromycin gene for eukaryotic selection and a cytomegalovirus promoter-

driven enhanced green fluorescence gene was used as a basis for the targeting vector (B951) (4). B951 was flanked with two half terminal repeats to generate the targeting vector. Ten million marmoset B-cells transformed by the virus that infects sLCL-2 were electroporated with 10µg of the targeting vector (270V, 960µF) and incubated in 10 ml RPMI 20% FBS for 16 hr at 37°C. 10^4 cells per well were plated onto 96-U-well plates in RPMI 10% FBS + 75µg/ml hygromycin. Four weeks later, circular DNA from 15 hygromycin-resistant clones was prepared and transformed into *E. coli* DH10B strain (41). DNA from cam-resistant colonies (15 µg/ml) was prepared and cleaved with the BamHI restriction enzyme. BAC DNA from one of these clones (B048, dubbed rMSHJ) contained a complete genome whose restriction pattern was partly similar to the one observed in the recombinant B95-8 and M81 strains. This DNA was amplified and transfected into HEK293 cells (1µg DNA per $4x10^5$ cells) using lipofection (Metafectene; Biontex). Cells were seeded onto 150 mm culture plates in RPMI supplemented with 10% FBS and hygromycin (100 µg/ml). Multiple GFP-positive colonies were expanded four weeks post-transfection and tested for their ability to produce virus particles upon induction of the lytic cycle. The recombinant B95-8 and M81 BAC clones were previously described (4).

Sequencing and alignment

The B048 clone was sequenced by high throughput sequencing with an Illumina HiSeq 2000 and assembled using the GS Reference Mapper software. This analysis showed that the recombination occurred between the TR from MSHJ and M81 between the nucleotides 101 and 344 from MSHJ and nucleotides 83 and 326 from the M81 TR. The sequences of the ambiguous regions and the repeat regions were further confirmed

using a standard Sanger sequencing method. The sequences of the MSHJ and IM-3 genomes are available (GenBank accession numbers MK973062 and MK973061).

To perform alignments, the currently available EBV genome sequences were downloaded from the NCBI database. The EBV genomes were aligned with the Multiple Alignment using Fast Fourier Transform (MAFFT) v7.419 software (42). The phylogenic tree was generated with the MEGA7 software using minimum-evolution method.

Gardella Gel Electrophoresis and Southern Blot Analysis.

Cell lines were analyzed for evidence of linear or episomal viral DNA using the agarose gel electrophoresis described by Gardella et al. (43). In this method, 5x10E5 infected B-cells were lysed in gel slots to avoid shearing of the viral DNA they carry. Southern blot hybridization was performed as described before using a P32-labeled probe directed against non-repetitive sequences specific to the EBV gp350 gene locus (44).

Immunostaining and Western Blot

Cells were fixed with 4% paraformaldehyde (BZLF1, EBNA2) or acetone (gp350) for 20 min at room temperature. PFA-fixed cells were permeabilized in PBS 0.5% Triton X-100 for 2 min. Fixed cells were incubated with the first antibody at 37°C for 30 min, washed in PBS thrice, and incubated at 37°C for 30 min with the secondary antibody conjugated to Cy-3. Slides were embedded with 90% glycerol and visualized with a Leica DM5000B epifluorescence microscope. Western blots for viral proteins were performed as described before (45). For detection of EBNA1, -2, -3A/B/C, BZLF1, PARP and LMP-1, 50 µg of total proteins were denatured with beta-mercaptoethanol and loaded onto a 10% or a 12.5% SDS acrylamide gel. For detection of gp350, 50 µg

of non-denatured proteins were loaded onto a 7.5% SDS acrylamide gel. The list of antibodies used in this study is given in Table 6.

Electron Microscopy

6x10E6 cells were centrifuged for 10 min at 400 rpm. Further preparation, embedding, and sections were carried out as described previously (46). Ultrathin sections were examined by electron microscopy (Zeiss, EM900).

Virus Production

For recombinant virus production, lytic replication of 293/rMSHJ, 293/rM81, 293/rB95-8 was induced by transfection of a BZLF1 expression plasmid with or without cotransfection of a BALF4 expression plasmid as described previously (45). The supernatants were collected four days post-transfection and filtered through a 0.45µm filter to remove cell debris.

qPCR

We performed qPCR to determine the EBV viral load in supernatants from producer cell lines. Briefly, 44 µl of the tested samples were treated with 1 unit of DNase I at 37°C for one hour to destroy free viral DNA, followed by a heat inactivation step at 70°C for 10 min. Proteinase K was then added at a concentration of 0.1 mg/ml for one hour at 50°C and heat-inactivated at 75°C for 20 min. Aliquots were diluted 1/10 with water and amplified by qPCR using primers and probes specific to the BALF5 DNA polymerase gene and a Taqman universal master mix as previously described (47). A standard curve was used to calculate EBV copy numbers per ml.

Virus Infections

B-cells purified from peripheral blood with CD19-specific antibodies were exposed to viral supernatant for two hours at a multiplicity of infection (MOI) of 10 viral genomes per B cell, then washed once with PBS and cultured with RPMI supplemented with 20% FBS in the absence of immunosuppressive drugs. Three days after infection, an EBNA2 staining was performed, 3 EBNA2-positive B-cells/well were seeded into 48 wells of 96-U-well plates that contained 10xE3 gamma-irradiated NHDF feeder cells. We included non-infected B-cells as a negative control. Outgrowth of lymphoblastoid cell clones was monitored for 30 days post infection. Viruses used for infection of primary epithelial cells or of NSG-A2 mice were obtained by ultra-centrifugation of infectious supernatants (30000 x g for 2 hr at 4°C with a TLA-110 Beckman rotor) and resuspended in PBS. Transfer infection of primary epithelial cells was performed by coculture with primary B-cells previously exposed to viral supernatants at a MOI of 100 for 2 hr at room temperature and left in RPMI-20% FBS for 20 hr in a CO_2 incubator (17). Virus-loaded B-cells were then washed once in culture medium used for primary epithelial cells (KGM-SFM, invitrogen) and cocultured with primary epithelial cells at a concentration of 3 virus-loaded B-cells per epithelial cell. The B-cells were carefully removed 24 hr post-seeding and the infection rate of the primary epithelial cells was determined 48 hr thereafter by *in situ* hybridization with an EBER-specific PNA probe in conjunction with a PNA ISH detection kit (Dako) according to the manufacturers' protocol.

Transformation experiments in non-humanized NSG mice

We isolated human $CD19^+$ B-cells from buffy coats and exposed them to virus supernatants at a multiplicity of infection sufficient to generate 20% of EBNA2-positive

cells for 2 hours at room temperature under constant agitation (18). The infected cells were collected by centrifugation and washed twice with PBS. 2x10E6 of these cells, equivalent to 4x10E5 infected cells, were injected intraperitoneally into NSG mice (18). The mice were euthanized at 5 weeks post-injection, autopsied and their organs were subjected to macroscopic and microscopic investigation.

Immunohistochemistry

Organs from the euthanized NSG mice were fixed in 10% formalin and embedded in paraffin, and 3-µm-thin sections were prepared and immunostained after antigen retrieval (10 mM sodium citrate, 0.05% Tween 20 (pH 6.0), 99°C for 45 min). Bound antibodies were visualized with the Envision+ Dual link system-HRP (Dako). Pictures were taken with a camera attached to a light microscope (Leica DM2500). Measurements on stained tissues were performed with the Leica application Suite X software. Paired Student's t-tests were performed with GraphPad PRISM 8.0 to assess the statistical significance of the results.

Chemical inducers and calcium signaling

1x10E5 cells from the panel of spontaneous LCLs and of B-cells transformed by rB95-8, rM81 or rMSHJ were seeded into one well of a 96-well plate and incubated for 3 days with ionomycin (1µg/ml), TPA (20ng/ml)/Butyrate (3.3mM) or TGF-ß (0.5ng/ml). In another sets of experiments, cells were treated with cyclosporin A (CSA, 1µg/ml), with anti-human B cell receptor antibodies (IgG/A/M (H+L) F(ab')2 fragment (Sigma, 20µg/ml), with Rapamycin (10mM) or Ibrutinib (10nM and 100nM) for seven days. A 10nM concentration of Ibrutinib fully inactivates the BTK active site (19). After seven days, an immunofluorescent staining for BZLF1 was performed and the number of

positive cells determined by counting. The experiment was performed in triplicate and included mock-treated cells as a control.

Cell lines

HEK293 is a neuroendocrine cell line obtained by transformation of embryonic epithelial kidney cells with adenovirus (48). Peripheral blood $CD19^+$ B-cells were isolated from fresh buffy coats by ficoll density gradient followed by selection with anti-CD19 PanB Dynabeads and detachment of the beads as recommended by the manufacturer (Invitrogen). These cells were exposed to various viruses to generate new virus-transformed cell lines (daughter cells). LCLs and cell lines were routinely cultured in RPMI-1640 medium (Invitrogen) supplemented with 10% fetal bovine serum (FBS) (Biochrom).

Hypoxia treatment

1x10E5 cells from the rB95-8, rM81 and rMSHJ cell lines were seeded into one well of a 96-well plate and maintained under hypoxic conditions (O_2 1.0%) in an InvivO2 workstation (Baker) for one, three, five or seven days. Cells kept under non-hypoxic atmospheric O_2 concentrations (CO_2 5%) served as a control. The experiment was performed in triplicate at 35- and 90- days post infection.

605 **Acknowledgments**

606 We thank the staff of the DKFZ animal facility, the High Throughput Sequencing unit,
607 the Central Unit for Electron Microscopy and the Imaging and Cytometry core facility
608 at DKFZ for excellent technical support.

609

610 Ming-Han Tsai is supported by the Ministry of Science and Technology, Taiwan
611 (MOST-108-2636-B-010-001). SD was supported by a maternity leave by the DZIF.

612

Figure legends

Figure 1 Multiple EBV-positive B cell lines from western individuals support lytic replication

Twenty-two sLCLs were immunostained with antibodies specific for BZLF1 and gp350. The pictures show the results of the staining in two of the investigated cases, together with cells infected with rM81 (white arrows: gp350-positive cells, white arrowhead: cells covered with viruses). The graphs give the percentage of BZLF1- and gp350-positive replicating cells, to the exclusion of non-replicating cells coated with viruses.

Figure 2 Multiple EBV-positive B cell lines from western individuals produce viruses

A) A Gardella gel analysis was performed to identify linear viral DNA that is produced during lytic replication. M81 served as a positive control, Raji as a negative control. B) Electron microscopy pictures showing viruses at the surface of EBV-positive B-cells in five cell lines. C) The panel of cell lines was subjected to a western blot analysis with a gp350-specific probe. The EBV-negative Elijah cell line served as a negative control.

Figure 3 The ability of virus isolates to replicate is maintained in different B cell populations and chemical induction of lytic replication

A) Thirteen iEBVL and IM sLCLs produced enough virus to infect another unrelated B cell sample. The replication rate as assessed by the percentage of BZLF1-positive B-cells in the parental and in daughter cell lines is given in a dot plot. The average and standard error is also indicated. B) We also show an example of an immunofluorescence staining and a western blot for gp350 in parental and daughter cells. C) (Right panel).

Fifteen spontaneous LCLs were treated with a combination of TPA and butyrate, TGF-beta, or ionomycine. The left dot plot shows the fold change in the number of BZLF1-positive B-cells after exposure to the first two drugs, relative to mock-treated cells, the right dot plot shows the percentage of BZLF1-positive B-cells in the presence of absence of ionomycine. D) Three independent primary B cell samples transformed with rMSHJ, rM81 and rB95-8 were treated with antibodies directed against the B cell receptor, ionomycin (Left panel) or cyclosporin A (Right panel). The dot plots show the fold change in the number of BZLF1-positive B-cells, relative to mock-treated cells.

Figure 4 MSHJ replication in marmoset cell lines and its cloning as a BAC

A) Primary B-cells from the peripheral blood of marmosets were infected with sLCL-2. B-cells infected by rM81 or by rB95-8 served as positive and negative controls, respectively. The picture shows BZLF1 and gp350-positive cells (red), the first graph gives the percentage of positive cells in the cell lines and the second gives the viral titers in the supernatants of the cell lines, as determined by qPCR.

B) The rMSHJ, rM81 and rB95-8 genomes were digested with BamHI and the resulting fragments separated onto an agarose gel. The size of the fragments is given by the DNA ladders.

Figure 5 IM-3 and rMSHJ are closely related to B95-8

The genome of IM-3 and MSHJ (indicated by a dot) were aligned to 130 published EBV genomes, including B95-8 (indicated by a square). The genetic tree shows the degree of divergence between the sequences, the numbers give the branch length percentage and thus the level of divergence.

Figure 6 rMSHJ B cell tropism and transformation efficiency

A) Three independent sets of primary B-cells were infected with rMSHJ, rM81 and rB95-8 at the same multiplicity of infection (10 genome equivalents per cell). Three days later, cells were stained for the EBNA2 protein. The dot plot shows the percentage of infected B-cells. B) Three independent sets of primary B-cells were infected with rMSHJ, rM81 and rB95-8 at the same multiplicity of infection (10 genome equivalents per cell). Three days after infection, cells were stained for EBNA2. Infected cells were seeded in a 96 well cluster plate at a concentration of three EBNA2-positive per well. Five weeks later, the percentage of outgrown wells was determined. The results are given in the dot plots. C) 3x10E5 cells from LCLs generated with rMSHJ, rM81 and rB95-8 were kept in culture for four weeks to generate a growth curve that is reproduced in the graph.

Figure 7 rMSHJ epitheliotropism

Primary epithelial cells were infected with rMSHJ, rM81 and rB95-8 at the same multiplicity of infection (100 genome equivalents per cell) using either direct or transfer infection on primary B-cells. Three days later, cells were subjected to in situ hybridization with a probe specific for the highly abundant non-coding RNA EBER. A) shows a representative example of transfer infection. B) The graph of bars shows the percentage of infected cells under the different conditions studied after infection of 3 samples. Cells were infected with viruses that express gp110 at high or low levels. We give the mean and standard error from three infection experiments.

Figure 8 B-cells infected with rMSHJ undergo a high level of spontaneous lytic replication.

Three sets of independent primary B cell samples were infected with rMSHJ, rM81 and rB95-8. Expression of BZLF1 and gp350 was monitored once a week for four weeks. A) shows an example of immunostaining with BZLF1 and gp350. BZLF1 signals were detected in the nucleus, but also in the cytoplasm (white arrowheads) of infected cells. The dotplots show the percentage of cells displaying nuclear (left) or cytoplasmic (right) over time. B) Six weeks after infection, infected cells were subjected to immunofluorescence staining with antibodies specific for BZLF1 and gp350. The percentage of positive cells is given in the dot plots, together with the standard error. C) BZLF1 and gp350 expression in one B cell sample infected with the three viruses as determined by western blot. Staining for actin expression was used as a loading control. D) The pictures show expression of BZLF1 and gp350 in EBV-positive lymphoid tumors that developed in immunosuppressed mice after infection with rM81 or rMSHJ.

Figure 9 B-cells infected with rMSHJ are sensitive to ibrutinib and rapamycin treatment.

A) Three independent primary B cell samples transformed with rMSHJ, rM81 and rB95-8 were exposed to Ibrutinib (10 nM, 100 nM) or rapamycin (10 nM). B) Western blot showing expression p-Btk and pAKT-1 in rB95.8-transformed B cells with or without 10 nM Ibrutinib treatment (upper panel). Western blot showing p-Btk expression in B cells transformed by various viral strains S1 and S2: blood samples 1 and 2 (lower panel). C) Viability of 4 EBV-transformed B cell samples (LCL1 to 4) after treatment with increasing concentrations of Ibrutinib or Rapamycin D) Cell growth

rate of an EBV-transformed B cell sample after treatment with different concentrations of Ibrutinib or Rapamycin.

Figure 10 Hypoxia reactivates lytic replication and lytically replicating cells are located closed to capillaries.

A) Three independent primary B cell samples, each transformed with rMSHJ, rM81 and rB95-8 were kept under hypoxia for up to 7 days. The percentage of BZLF1-positive cells was determined after 1, 3, 5 and 7 days of hypoxia. The experiment was performed with 30- (left panel) or 90-days old transformed B cell samples (right panel). One 90-day old cell sample set was analyzed by western blot using antibodies specific to BZLF1, gp350, LMP1, EBNA2, actin and PARP after hypoxia treatment.

B) Immunohistochemistry showing CD34-positive small arteries (white arrowhead) and capillaries (arrow), together with BZLF1-positive B-cells (arrowhead). We show one sample infected with rM81 and one sample infected with rMSHJ at low (x20) and high (x40) power. C) We measured the shortest distance between 100 BZLF1-positive B-cells and the closest capillary or small artery. The results are given as dotplots for tissues infected with rM81 (left) and rMSHJ (right).

References

1. Rickinson AB, Kieff E. 2007. Epstein-Barr virus, p 2655-2700. *In* Knipe DM, Howley PM, Griffin DE, Lamb RA, Martin MA, Roizman B, Strauss SE (ed). Lippincott Williams & Wilkins, Philadelphia.

2. Dolcetti R, Dal Col J, Martorelli D, Carbone A, Klein E. 2013. Interplay among viral antigens, cellular pathways and tumor microenvironment in the pathogenesis of EBV-driven lymphomas. Semin Cancer Biol 23:441-56.

3. Klinke O, Feederle R, Delecluse HJ. 2014. Genetics of Epstein-Barr virus microRNAs. Semin Cancer Biol 26:52-9.

4. Tsai M-H, Raykova A, Klinke O, Bernhardt K, Gärtner K, Leung CS, Geletneky K, Sertel S, Münz C, Feederle R, Delecluse H-J. 2013. Spontaneous lytic replication and epitheliotropism define an Epstein-Barr virus strain found in carcinomas. Cell reports 5:458-70.
5. Coghill AE, Hildesheim A. 2014. Epstein-Barr virus antibodies and the risk of associated malignancies: review of the literature. Am J Epidemiol 180:687-95.
6. Chien YC, Chen JY, Liu MY, Yang HI, Hsu MM, Chen CJ, Yang CS. 2001. Serologic markers of Epstein-Barr virus infection and nasopharyngeal carcinoma in Taiwanese men. N Engl J Med 345:1877-82.
7. Montone KT, Hodinka RL, Salhany KE, Lavi E, Rostami A, Tomaszewski JE. 1996. Identification of Epstein-Barr virus lytic activity in post-transplantation lymphoproliferative disease. Mod Pathol 9:621-30.
8. Rea D, Delecluse HJ, Hamilton-Dutoit SJ, Marelle L, Joab I, Edelman L, Finet JF, Raphael M. 1994. Epstein-Barr virus latent and replicative gene expression in post-transplant lymphoproliferative disorders and AIDS-related non-Hodgkin's lymphomas. French Study Group of Pathology for HIV-associated Tumors. Ann Oncol 5 Suppl 1:113-6.
9. Shumilov A, Tsai MH, Schlosser YT, Kratz AS, Bernhardt K, Fink S, Mizani T, Lin X, Jauch A, Mautner J, Kopp-Schneider A, Feederle R, Hoffmann I, Delecluse HJ. 2017. Epstein-Barr virus particles induce centrosome amplification and chromosomal instability. Nat Commun 8:14257.
10. Delecluse S, Yu J, Bernhardt K, Haar J, Poirey R, Tsai MH, Kiblawi R, Kopp-Schneider A, Schnitzler P, Zeier M, Dreger P, Wuchter P, Bulut OC, Behrends U, Delecluse HJ. 2019. Spontaneous lymphoblastoid cell lines from patients with Epstein-Barr virus infection show highly variable proliferation characteristics that correlate with the expression levels of viral microRNAs. PLoS One 14:e0222847.
11. McKenzie J, El-Guindy A. 2015. Epstein-Barr Virus Lytic Cycle Reactivation. Curr Top Microbiol Immunol 391:237-61.
12. Gutierrez MI, Ibrahim MM, Dale JK, Greiner TC, Straus SE, Bhatia K. 2002. Discrete alterations in the BZLF1 promoter in tumor and non-tumor-associated Epstein-Barr virus. J Natl Cancer Inst 94:1757-63.
13. Bristol JA, Djavadian R, Albright ER, Coleman CB, Ohashi M, Hayes M, Romero-Masters JC, Barlow EA, Farrell PJ, Rochford R, Kalejta RF, Johannsen EC, Kenney SC. 2018. A cancer-associated Epstein-Barr virus BZLF1 promoter variant enhances lytic infection. PLoS Pathog 14:e1007179.
14. Palser AL, Grayson NE, White RE, Corton C, Correia S, Ba Abdullah MM, Watson SJ, Cotten M, Arrand JR, Murray PG, Allday MJ, Rickinson AB, Young LS, Farrell PJ, Kellam P. 2015. Genome diversity of Epstein-Barr virus from multiple tumor types and normal infection. J Virol 89:5222-37.
15. Gratama JW, Oosterveer MA, Weimar W, Sintnicolaas K, Sizoo W, Bolhuis RL, Ernberg I. 1994. Detection of multiple 'Ebnotypes' in individual Epstein-Barr virus carriers following lymphocyte transformation by virus derived from peripheral blood and oropharynx. J Gen Virol 75 (Pt 1):85-94.
16. Feederle R, Neuhierl B, Bannert H, Geletneky K, Shannon-Lowe C, Delecluse HJ. 2007. Epstein-Barr virus B95.8 produced in 293 cells shows marked tropism for differentiated primary epithelial cells and reveals interindividual variation in susceptibility to viral infection. Int J Cancer 121:588-94.

792 17. Shannon-Lowe CD, Neuhierl B, Baldwin G, Rickinson AB, Delecluse HJ. 2006.
793 Resting B cells as a transfer vehicle for Epstein-Barr virus infection of epithelial
794 cells. Proc Natl Acad Sci U S A 103:7065-70.
795 18. Lin X, Tsai MH, Shumilov A, Poirey R, Bannert H, Middeldorp JM, Feederle R,
796 Delecluse HJ. 2015. The Epstein-Barr Virus BART miRNA Cluster of the M81 Strain
797 Modulates Multiple Functions in Primary B Cells. PLoS Pathog 11:e1005344.
798 19. Brown JR. 2013. Ibrutinib (PCI-32765), the first BTK (Bruton's tyrosine
799 kinase) inhibitor in clinical trials. Curr Hematol Malig Rep 8:1-6.
800 20. Kosowicz JG, Lee J, Peiffer B, Guo Z, Chen J, Liao G, Hayward SD, Liu JO,
801 Ambinder RF. 2017. Drug Modulators of B Cell Signaling Pathways and Epstein-
802 Barr Virus Lytic Activation. J Virol 91.
803 21. Adamson AL, Le BT, Siedenburg BD. 2014. Inhibition of mTORC1 inhibits
804 lytic replication of Epstein-Barr virus in a cell-type specific manner. Virol J 11:110.
805 22. Kraus RJ, Yu X, Cordes BA, Sathiamoorthi S, Iempridee T, Nawandar DM, Ma
806 S, Romero-Masters JC, McChesney KG, Lin Z, Makielski KR, Lee DL, Lambert PF,
807 Johannsen EC, Kenney SC, Mertz JE. 2017. Hypoxia-inducible factor-1alpha plays
808 roles in Epstein-Barr virus's natural life cycle and tumorigenesis by inducing lytic
809 infection through direct binding to the immediate-early BZLF1 gene promoter.
810 PLoS Pathog 13:e1006404.
811 23. Lucker A, Weber B, Jenny P. 2015. A dynamic model of oxygen transport
812 from capillaries to tissue with moving red blood cells. Am J Physiol Heart Circ
813 Physiol 308:H206-16.
814 24. Fina L, Molgaard HV, Robertson D, Bradley NJ, Monaghan P, Delia D,
815 Sutherland DR, Baker MA, Greaves MF. 1990. Expression of the CD34 gene in
816 vascular endothelial cells. Blood 75:2417-26.
817 25. Miller G, Robinson J, Heston L, Lipman M. 1974. Differences between
818 laboratory strains of Epstein-Barr virus based on immortalization, abortive
819 infection, and interference. Proc Natl Acad Sci U S A 71:4006-10.
820 26. Davies ML, Xu S, Lyons-Weiler J, Rosendorff A, Webber SA, Wasil LR, Metes
821 D, Rowe DT. 2010. Cellular factors associated with latency and spontaneous
822 Epstein-Barr virus reactivation in B-lymphoblastoid cell lines. Virology 400:53-67.
823 27. Sculley TB, Moss DJ, Hazelton RA, Pope JH. 1987. Detection of Epstein-Barr
824 virus strain variants in lymphoblastoid cell lines 'spontaneously' derived from
825 patients with rheumatoid arthritis, infectious mononucleosis and normal controls.
826 J Gen Virol 68 (Pt 8):2069-78.
827 28. Babcock GJ, Decker LL, Freeman RB, Thorley-Lawson DA. 1999. Epstein-
828 barr virus-infected resting memory B cells, not proliferating lymphoblasts,
829 accumulate in the peripheral blood of immunosuppressed patients. J Exp Med
830 190:567-76.
831 29. Qu L, Green M, Webber S, Reyes J, Ellis D, Rowe D. 2000. Epstein-Barr virus
832 gene expression in the peripheral blood of transplant recipients with persistent
833 circulating virus loads. J Infect Dis 182:1013-21.
834 30. Hopwood PA, Brooks L, Parratt R, Hunt BJ, Bokhari M, Thomas JA, Yacoub
835 M, Crawford DH. 2002. Persistent Epstein-Barr virus infection: unrestricted latent
836 and lytic viral gene expression in healthy immunosuppressed transplant
837 recipients. Transplantation 74:194-202.
838 31. Burns DM, Tierney R, Shannon-Lowe C, Croudace J, Inman C, Abbotts B,
839 Nagra S, Fox CP, Chaganti S, Craddock CF, Moss P, Rickinson AB, Rowe M, Bell AI.

2015. Memory B-cell reconstitution following allogeneic hematopoietic stem cell transplantation is an EBV-associated transformation event. Blood 126:2665-75.
32. Fink S, Tsai MH, Schnitzler P, Zeier M, Dreger P, Wuchter P, Bulut OC, Behrends U, Delecluse HJ. 2017. The Epstein-Barr virus DNA load in the peripheral blood of transplant recipients does not accurately reflect the burden of infected cells. Transpl Int 30:57-67.
33. Buck M, Cross S, Krauer K, Kienzle N, Sculley TB. 1999. A-type and B-type Epstein-Barr virus differ in their ability to spontaneously enter the lytic cycle. J Gen Virol 80 (Pt 2):441-5.
34. Vakiani E, Nandula SV, Subramaniyam S, Keller CE, Alobeid B, Murty VV, Bhagat G. 2007. Cytogenetic analysis of B-cell posttransplant lymphoproliferations validates the World Health Organization classification and suggests inclusion of florid follicular hyperplasia as a precursor lesion. Hum Pathol 38:315-25.
35. Bhende PM, Seaman WT, Delecluse HJ, Kenney SC. 2005. BZLF1 activation of the methylated form of the BRLF1 immediate-early promoter is regulated by BZLF1 residue 186. J Virol 79:7338-48.
36. Weiss ER, Lamers SL, Henderson JL, Melnikov A, Somasundaran M, Garber M, Selin L, Nusbaum C, Luzuriaga K. 2018. Early Epstein-Barr Virus Genomic Diversity and Convergence toward the B95.8 Genome in Primary Infection. J Virol 92.
37. Li Z, Tsai MH, Shumilov A, Baccianti F, Tsao SW, Poirey R, Delecluse HJ. 2019. Epstein-Barr virus ncRNA from a nasopharyngeal carcinoma induces an inflammatory response that promotes virus production. Nat Microbiol 4:2475-2486.
38. Desgranges C, Lenoir G, de-The G, Seigneurin JM, Hilgers J, Dubouch P. 1976. In vitro transforming activity of EBV. I-Establishment and properties of two EBV strains (M81 and M72) produced by immortalized Callithrix jacchus lymphocytes. Biomedicine 25:349-52.
39. Miller G, Shope T, Lisco H, Stitt D, Lipman M. 1972. Epstein-Barr virus: transformation, cytopathic changes, and viral antigens in squirrel monkey and marmoset leukocytes. Proc Natl Acad Sci U S A 69:383-7.
40. Pulvertaft JV. 1964. Cytology of Burkitt's Tumour (African Lymphoma). Lancet 1:238-40.
41. Griffin BE, Bjorck E, Bjursell G, Lindahl T. 1981. Sequence complexity of circular Epstein-Bar virus DNA in transformed cells. J Virol 40:11-9.
42. Katoh K, Misawa K, Kuma K, Miyata T. 2002. MAFFT: a novel method for rapid multiple sequence alignment based on fast Fourier transform. Nucleic Acids Res 30:3059-66.
43. Gardella T, Medveczky P, Sairenji T, Mulder C. 1984. Detection of circular and linear herpesvirus DNA molecules in mammalian cells by gel electrophoresis. J Virol 50:248-54.
44. Delecluse HJ, Hilsendegen T, Pich D, Zeidler R, Hammerschmidt W. 1998. Propagation and recovery of intact, infectious Epstein-Barr virus from prokaryotic to human cells. Proc Natl Acad Sci U S A 95:8245-50.
45. Neuhierl B, Feederle R, Hammerschmidt W, Delecluse HJ. 2002. Glycoprotein gp110 of Epstein-Barr virus determines viral tropism and efficiency of infection. Proc Natl Acad Sci U S A 99:15036-41.
46. Granato M, Feederle R, Farina A, Gonnella R, Santarelli R, Hub B, Faggioni A, Delecluse HJ. 2008. Deletion of Epstein-Barr virus BFLF2 leads to impaired viral

889 DNA packaging and primary egress as well as to the production of defective viral
890 particles. J Virol 82:4042-51.
891 47. Feederle R, Bannert H, Lips H, Muller-Lantzsch N, Delecluse HJ. 2009. The
892 Epstein-Barr virus alkaline exonuclease BGLF5 serves pleiotropic functions in
893 virus replication. J Virol 83:4952-62.
894 48. Shaw G, Morse S, Ararat M, Graham FL. 2002. Preferential transformation of
895 human neuronal cells by human adenoviruses and the origin of HEK 293 cells.
896 FASEB J 16:869-71.
897

Patient number	Age	Sex	Foreign country	Transplanted organ	Time from transplantation to increased EBVL (in days)	EBV cop/ml WB	Immunosuppressive regimen	PTLD	status at lat FU
sLCL-2	66	m	Germany	SCT	26	3150	CSA, MTX	-	alive
sLCL-3	56	f	Germany	KT	7456	9870	CSA, ST	yes*	alive
sLCL-4	66	f	Spain	KT	1821	18600	CSA, MMF, ST	-	alive
sLCL-5	64	m	Germany	SCT	29	1000	FK, MMF	-	dead (relapsed ALL)
sLCL-6	66	f	Germany	KT	3024	1730	ST	-	alive
sLCL-7	68	m	Germany	SCT	26	2390	CSA	-	alive
sLCL-8	46	f	Russia	SCT	41	2330	CSA	-	alive
sLCL-9	64	m	Germany	SCT	35	2600	CSA	-	alive
sLCL-10	60	f	Germany	KT	2853	1920	BELA/ST	-	alive
sLCL-11	63	m	Germany	SCT	273	16200	FK	-	alive
sLCL-12	32	m	Germany	KT	22	22600	CSA, ST	-	alive
sLCL-14	37	m	Germany	KT	810	16400	FK, MMF, ST	-	alive
sLCL-15	69	m	Germany	KT	613	1000	BELA, MMF	-	alive

Table 1. Characteristics of the studied patients (sLCL2 to-15) with an increased EBV load. EBVL: EBV load, CSA: cyclosporin A, MMF: mycophenolate mofetil, FK: tacrolimus, SIR: sirolimus, AZA: azathioprine, MTX: methotrexate, BELA: belatacept, KT: kidney transplantation, SCT: stem cell transplantation, ST: Steroid, m: male, f: female, cop: copies, WB: whole blood, FU: follow up, ALL: acute lymphoblastic leukemia. * T-cell PTLD not EBV-associated.

cell line	Mutations BZLF1 mini-Zp	Mutations BZLF1 ORF	closest EBV strain	EBV-type
sLCL-2	-	C696G	E1563 Owv7 (IM)	A
sLCL-3	-	-	B95-8 (IM)	A
sLCL-4	-	C188G	E1583 OWv7 (IM)	A
sLCL-5	-	C696G	E1563 Owv7 (IM)	A
sLCL-6	-	G616T C696G	GC-variant-9	A
sLCL-7	-	T383C G616T	GC-variant-9	A
sLCL-8	-	G616T	GC-variant-9	A
sLCL-9		-	B95-8 (IM)	A
sLCL-10	-	G616T	GC-variant-9	A
sLCL-11	-	A411C C696G	GK_BL67	A
sLCL-12	-	A471G	E1563 Owv7 (IM)	A
sLCL-14	-	A301C	B95-8 (IM)	A
sLCL-15	-	G616T	GC-variant-9	A
IM-1	-	C163T G616T	M-ABA	A
IM-2	-	-	B95-8 (IM)	A
IM-3	-	C696G	E1563 Owv7 (IM)	A
IM-4	-	-	B95-8 (IM)	A
IM-6	-	C169T G175A C181A T213C G403A T437C T459C A471G G613T	HL04	A
IM-7	-	C169T G175A C181A T213C G403A T437C T459C A471G G613T	HL04	A
IM-8	-	-	B95-8 (IM)	A
IM-9	-	C169T G175A C181A T213C G403A T437C T459C A471G G613T	HL04	
IM-10	-	G610T	GC-variant-9	A

Table 2. Polymorphisms in the BZLF1 gene and its promoter. IM: infectious mononucleosis, GC: gastric cancer, HL: Hodgkin lymphoma.

	IM-3	rMSHJ
number of bp differences compared to reference NC_007605_1	524	654
aligned sequence	135748	135744
closest IM-3 neighbour: sLCL-IS1.10 Australia PTLD	93	
closest rMSHJ neighbour: E1563_BCv1 USA IM		122
aligned sequence (tandem repeats are not considered)	135740	135741
number of bp differences between IM-3 and rMSHJ	280	
aligned sequence (tandem repeats are not considered)	135745	

Table 3. Non-synonymous mutations in rMSHJ and IM-3 relative to NC_007605_1. Base pairs = bp.

sequences with most polymorphisms	bp considered	polymorphisms			SNP + insertions/deletions	
		number of bp	%	amino-acids	number of SNP	insertions or deletions
region between BNLF2a ORF and LMP1 ORF	673	26	3,86		26	
oriP	1355	30	2,21		20	insertion 10 bp
EBNA1 ORF	1050	23	2,19	15	23	
BHRF1 intron	439	8	1,82		8	
Cp promoter (BCRF1 gene to Ws repeats)	1719	31	1,80		29	1 bp insertion, 1 bp deletion
EBNA2	1272	20	1,57	11	17	insertion 3 bp
LMP2A exon1	448	7	1,56	5	7	
BRRF2 ORF	1614	23	1,43	12	23	
LMP1 ORF	842	11	1,31	9	11	
RPSM1 promoter part between BART.I and BART.Ia	966	11	1,14		9	1 bp insertion, 1 bp deletion
BDLF3 ORF	705	7	0,99	3	7	
BBLF4 ORF	2430	20	0,82	5	20	
EBNA3C ORF+intron	2746	22	0,80	11	22	
BBLF2/BBLF3 ORF	2130	14	0,66	4	11	
BDLF2 ORF	1263	8	0,63	4	8	
BNRF1 ORF	3957	25	0,63	9	25	
BGLF3 ORF	999	6	0,60	1	6	
BRLF1 ORF	1818	10	0,55	4	10	
partial LMP2B gene (genome nt1-1691)	1691	9	0,53	1	9	
BGLF1 ORF	1521	7	0,46	2	4	deletion 3 bp
BPLF1 ORF	8700	37	0,43	15	37	
EBNA3A ORF	2835	11	0,39	7	11	
BBRF1 ORF	1842	7	0,38	1	7	
BOLF1 ORF	3720	12	0,32	4	9	insertion 3 bp
BSLF1 ORF	2625	4	0,15	1	6	
total:	**49360**	**389**		**124**	**365**	
% from total:	**36,4**	**74,2**			**69,7**	

Table 4. Polymorphisms of IM-3 relative to the reference NC_007605_1. Base pairs = bp, nucleotide = nt, open reading frame = ORF, single nucleotide polymorphism = SNP.

sequences with most polymorphisms	bp considered	polymorphisms			SNP + insertions/deletions	
		number of bp	%	amino-acids	number of SNP	insertions or deletions
EBER2 promoter before EBER2	74	4	5,41		4	
region between BNLF2a ORF and LMP1 ORF	673	19	2,82		19	
region between BMRF2 ORF and BSLF1 gene	537	15	2,79		14	insertion 1 bp
BDLF3 ORF	705	17	2,41	6	17	
oriP	1355	29	2,14		19	insertion 10 bp
EBNA1 ORF	1050	22	2,10	15	22	
BHRF1 intron	439	8	1,82		8	
Cp promoter (BCRF1 gene to Ws repeats)	1719	30	1,75		28	1 bp insertion, 1 bp deletion
LMP2A exon1	448	7	1,56	6	7	
BRRF2 ORF	1614	24	1,49	12	24	
LMP1 ORF	842	11	1,31	9	11	
EBNA2	1272	15	1,18	8	15	
RPSM1 promoter part between BART.1 and BART.Ia	966	11	1,14		8	1 bp insertion, 2 bp deletion
BGLF1 ORF	1521	17	1,12	2	14	deletion 3 bp
BDLF4 ORF	678	7	1,03	2	7	
BBLF4 ORF	2430	20	0,82	5	20	
BGLF3 ORF	999	8	0,80	1	8	
EBNA3C ORF+intron	2746	21	0,76	10	21	
BDLF1 ORF	906	6	0,66	1	6	
BBLF2/BBLF3 ORF	2130	14	0,66	4	14	
BDLF2 ORF	1263	8	0,63	4	8	
BNRF1 ORF	3957	25	0,63	9	25	
partial LMP2B gene (genome nt1-1691)	1691	10	0,59	1	10	
BXRF1 gene	2578	15	0,58	1	15	
BRLF1 ORF	1818	10	0,55	4	10	
BALF4 ORF	2574	12	0,47	4	12	
BcLF1 ORF	4146	19	0,46	2	19	
BPLF1 ORF	8652	37	0,43	15	37	
EBNA3A ORF	2835	11	0,39	7	11	
BBRF1 ORF	1842	7	0,38	1	7	
BOLF1 ORF	3723	12	0,32	4	9	insertion 3 bp
BSLF1 ORF	2625	6	0,23	2	6	
total:	**61263**	**477**		**135**	**464**	
% from total:	**45,2**	**72,9**			**69,6**	

Table 5. Polymorphisms of rMSHJ relative to the reference NC_007605_1. Base pairs = bp, nucleotide = nt, open reading frame = ORF, single nucleotide polymorphism = SNP.

antibody	clone	dilution	provider
gp350	72A1 (mouse, IF) OT6 (mouse, IHC)	1:30 1:600	R. Feederle JM. Middeldorp
BZLF1	BZ.1 (mouse)	1:200	R. Feederle
actin	ACTN05 (mouse)	1:10000	Dianova
LMP1	S12 (mouse)	1:4000	BD Pharmingen
EBNA2	PE2(mouse)	1:100	R. Feederle
EBNA1	IH4 (rat)	1:100	R. Feederle
LMP2A	15F9 (rat)	1:50	R. Feederle
EBNA3C	6C9 (rat)	1:100	R. Feederle
EBNA3B	A10-E3C (mouse)	1:100	R. Feederle
EBNA3A	E3AN-4A5 (rat)	1:100	R. Feederle
PARP	9542 (rabbit)	1:1000	Cell Signaling
CD34	EP373Y (rabbit)	1:200	Abcam

Table 6. Antibodies used. IF = immunofluorescence, IHC = immunohistochemistry

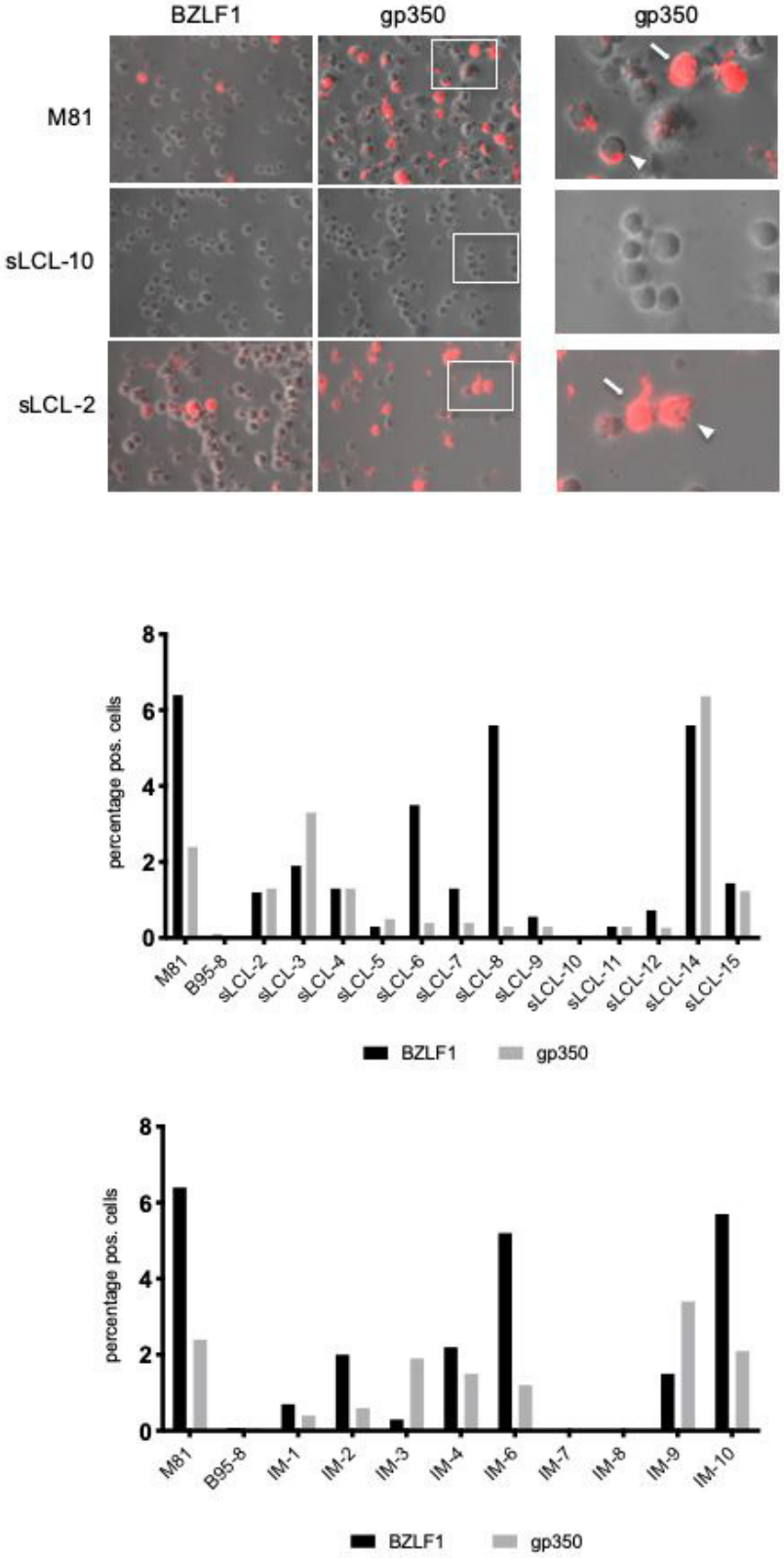

Figure 1

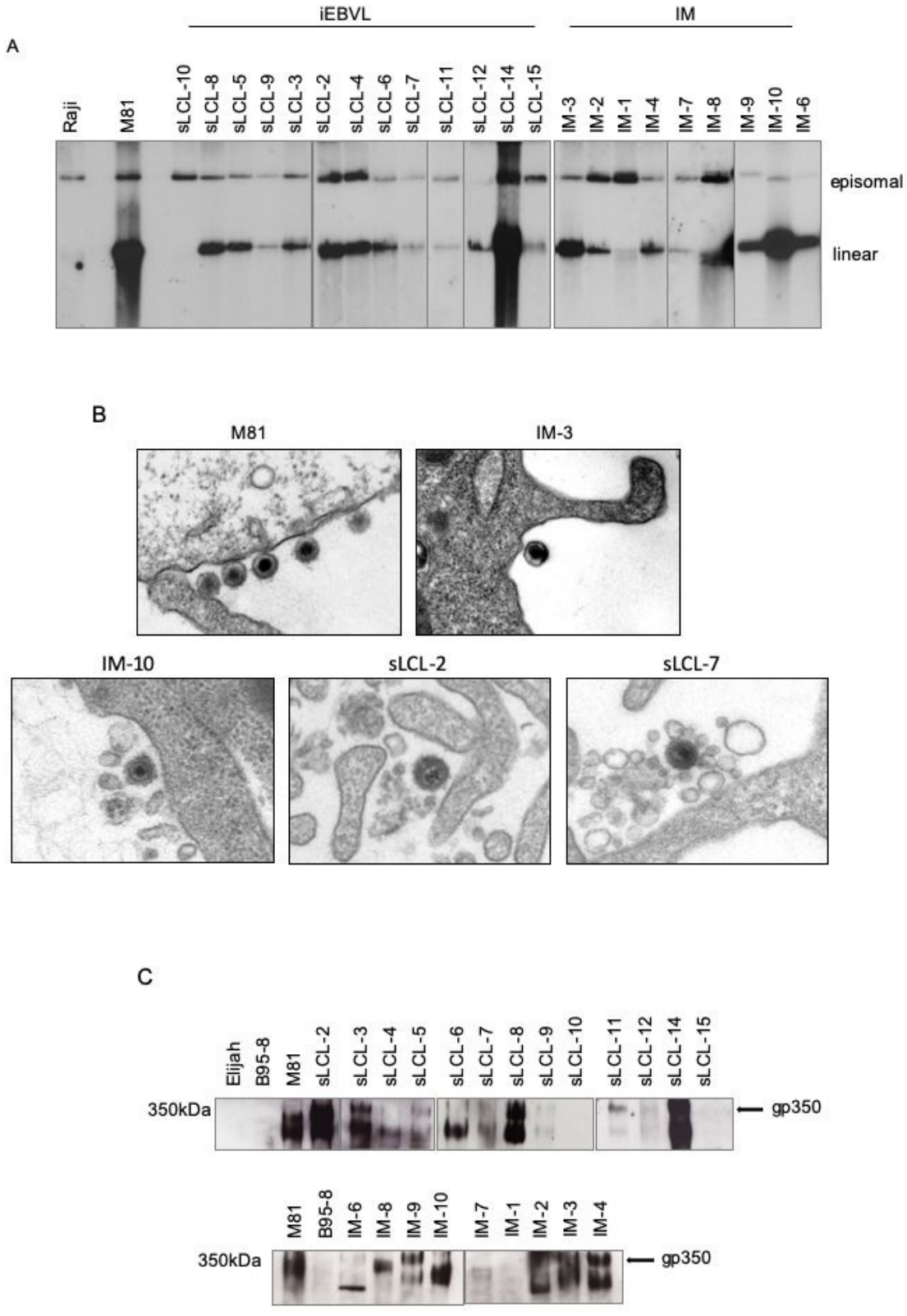

Figure 2

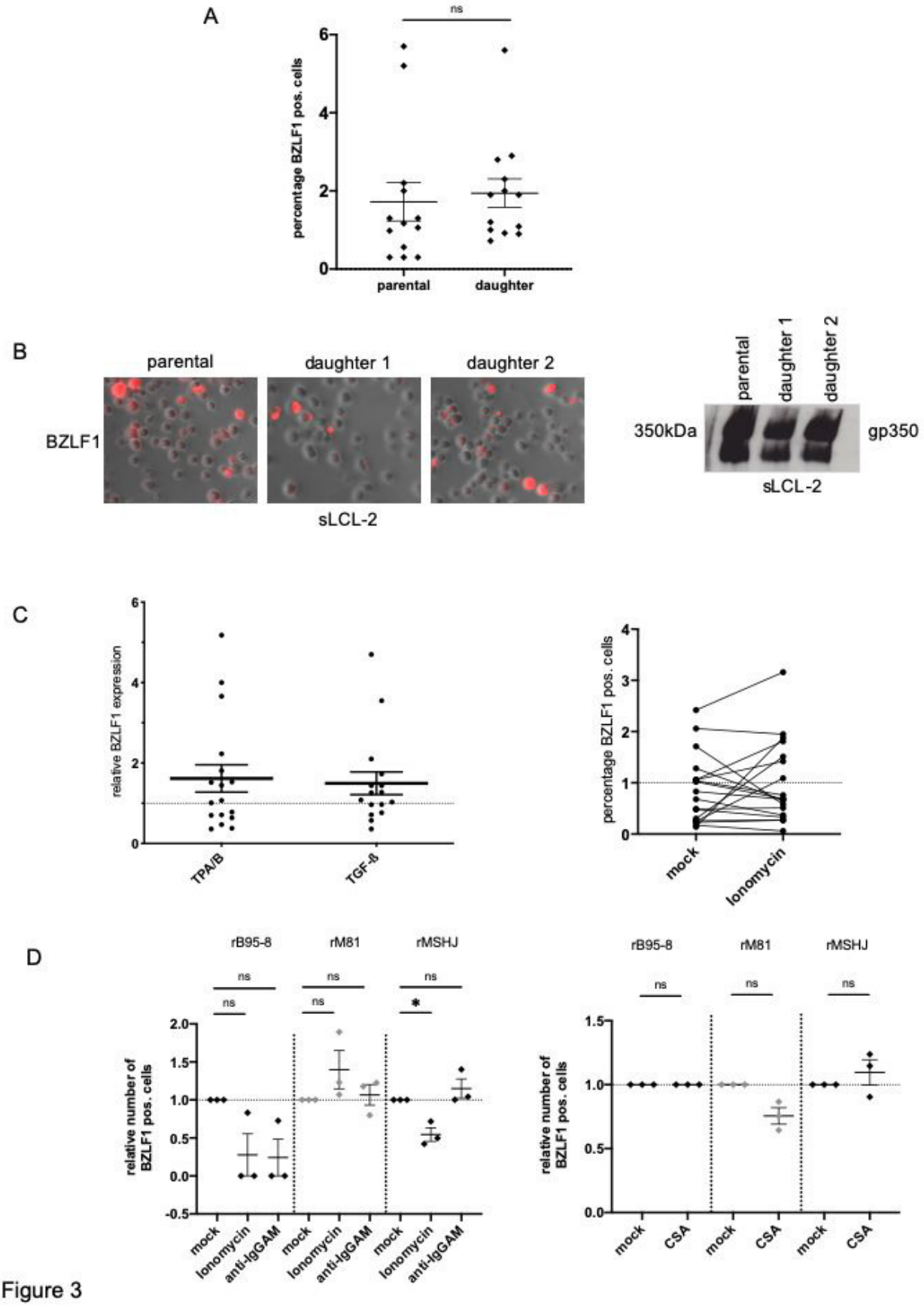

Figure 3

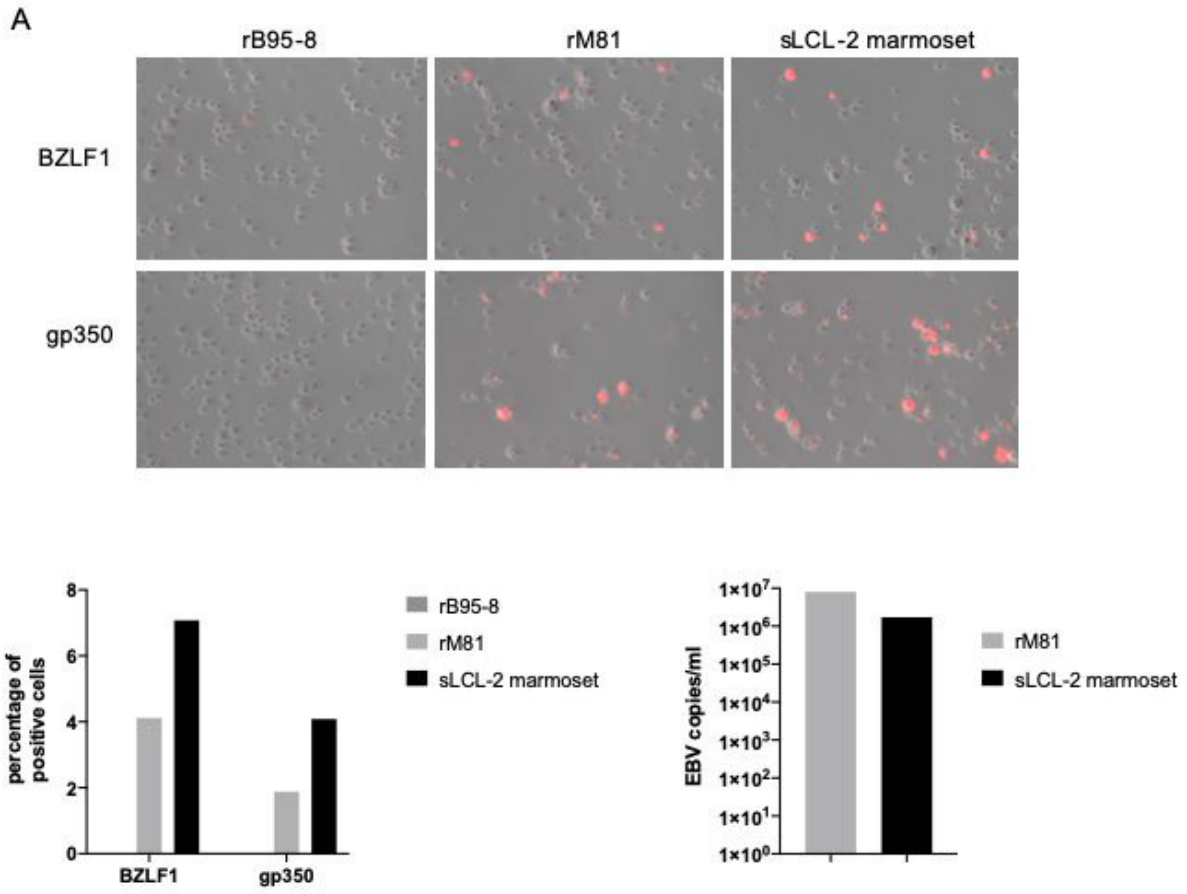

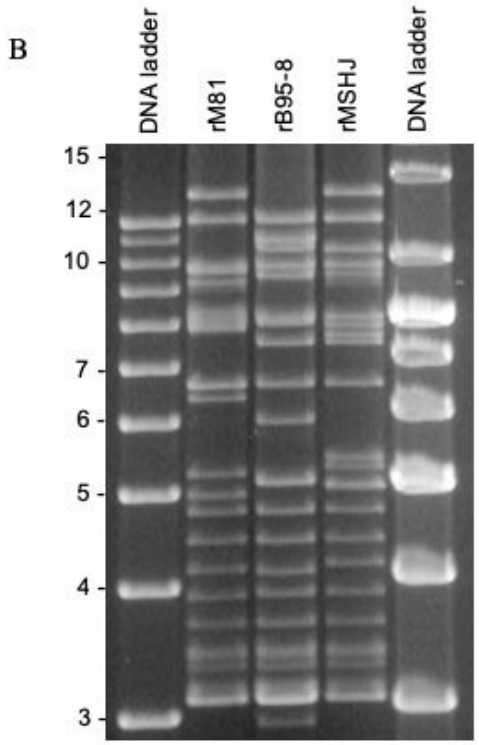

Figure 4

Figure 5

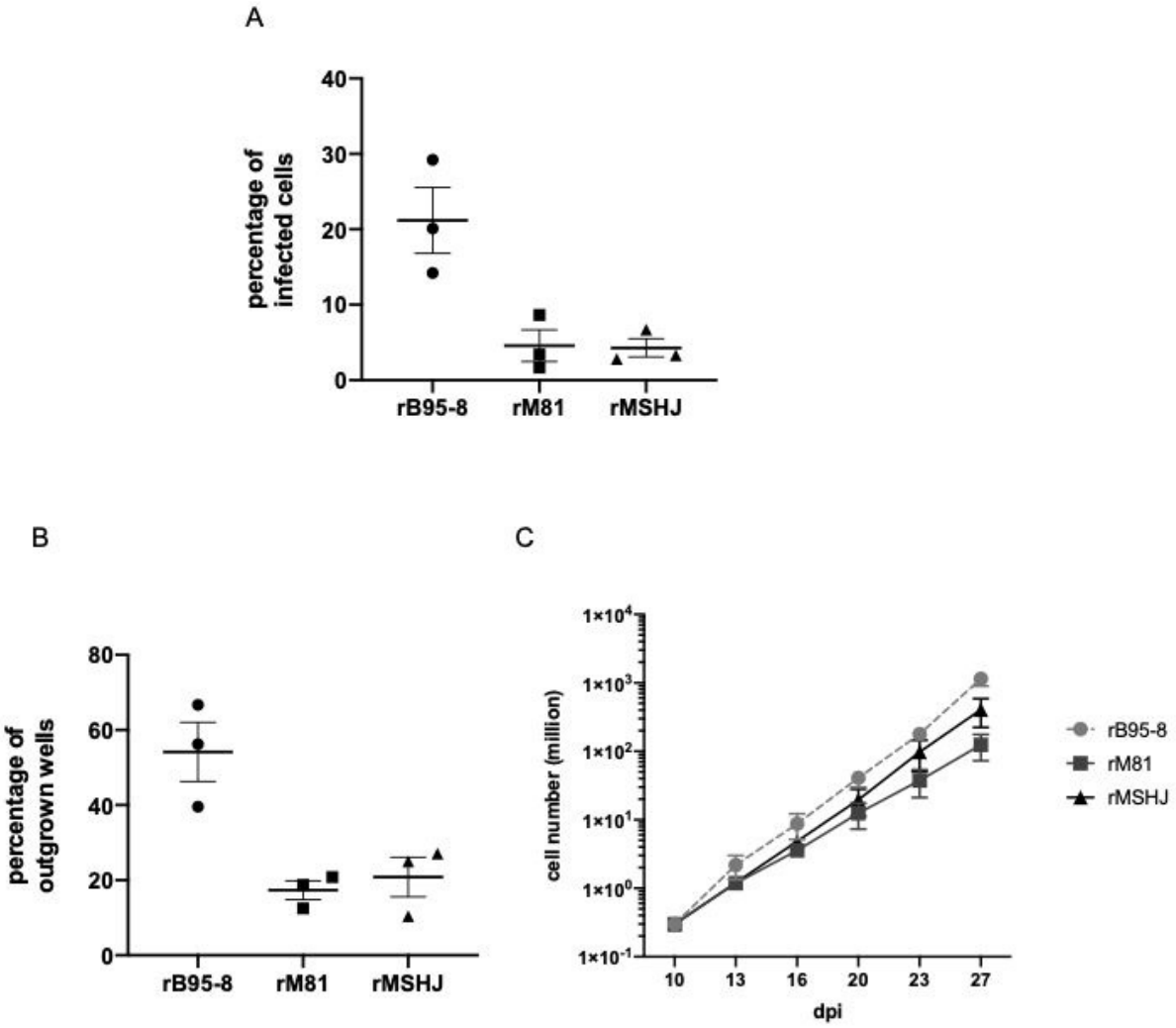

Figure 6

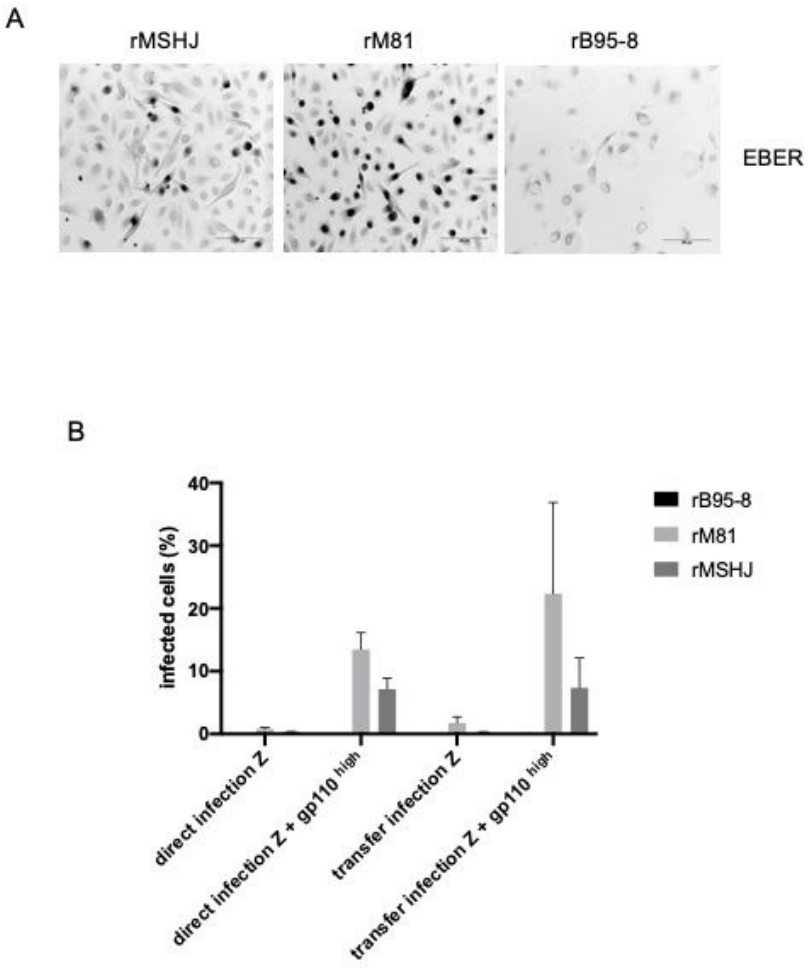

Figure 7

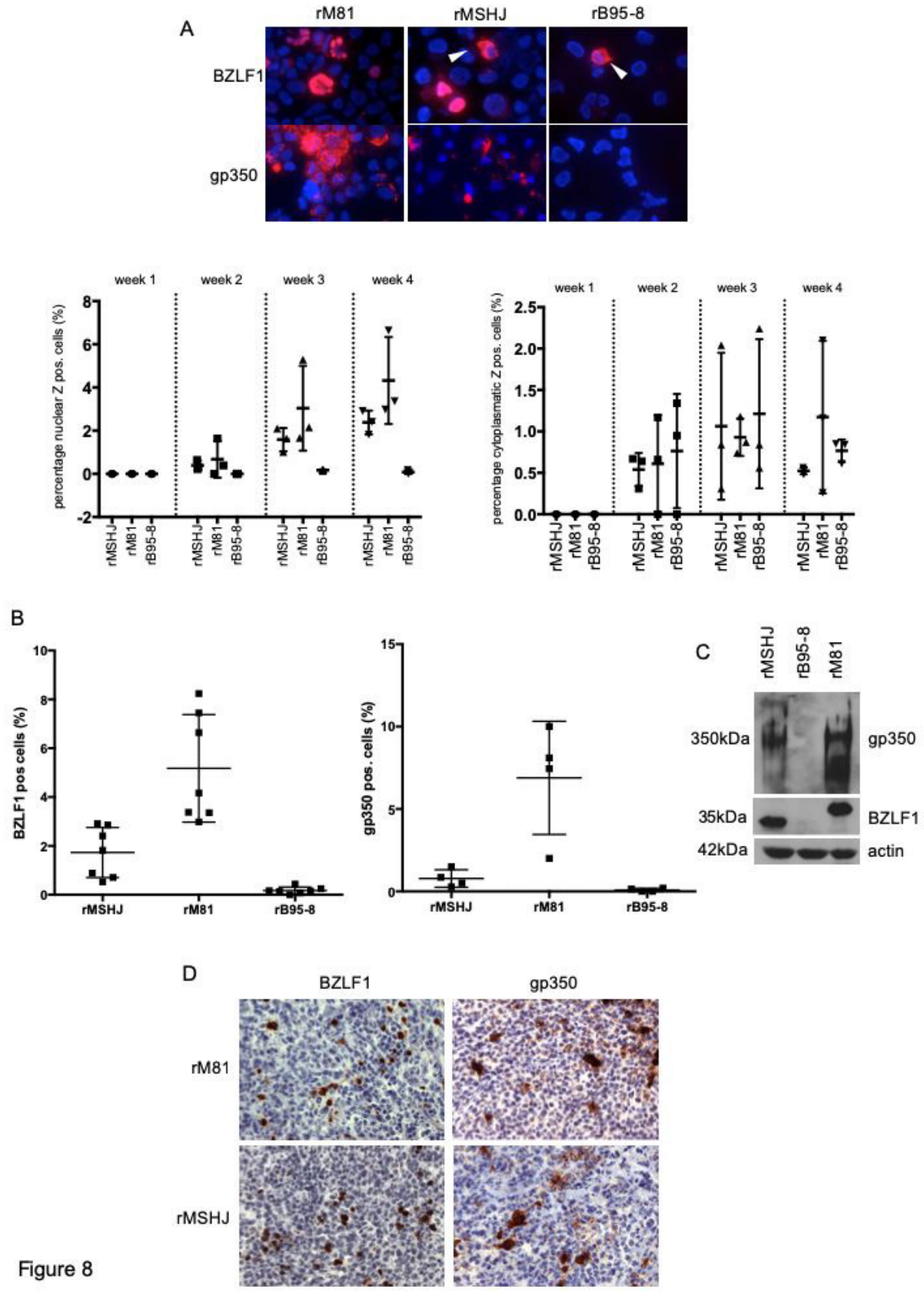

Figure 8

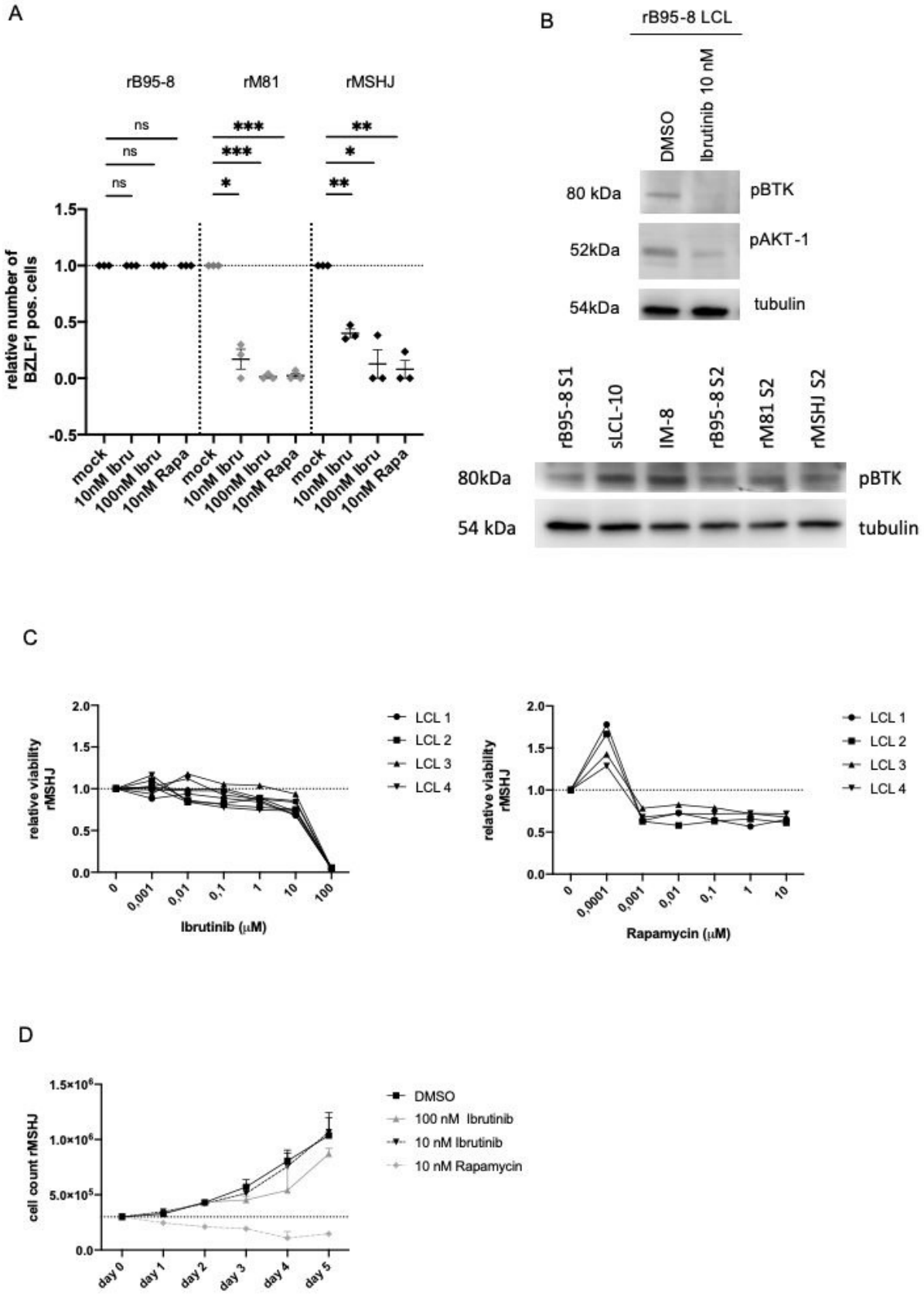

Figure 9

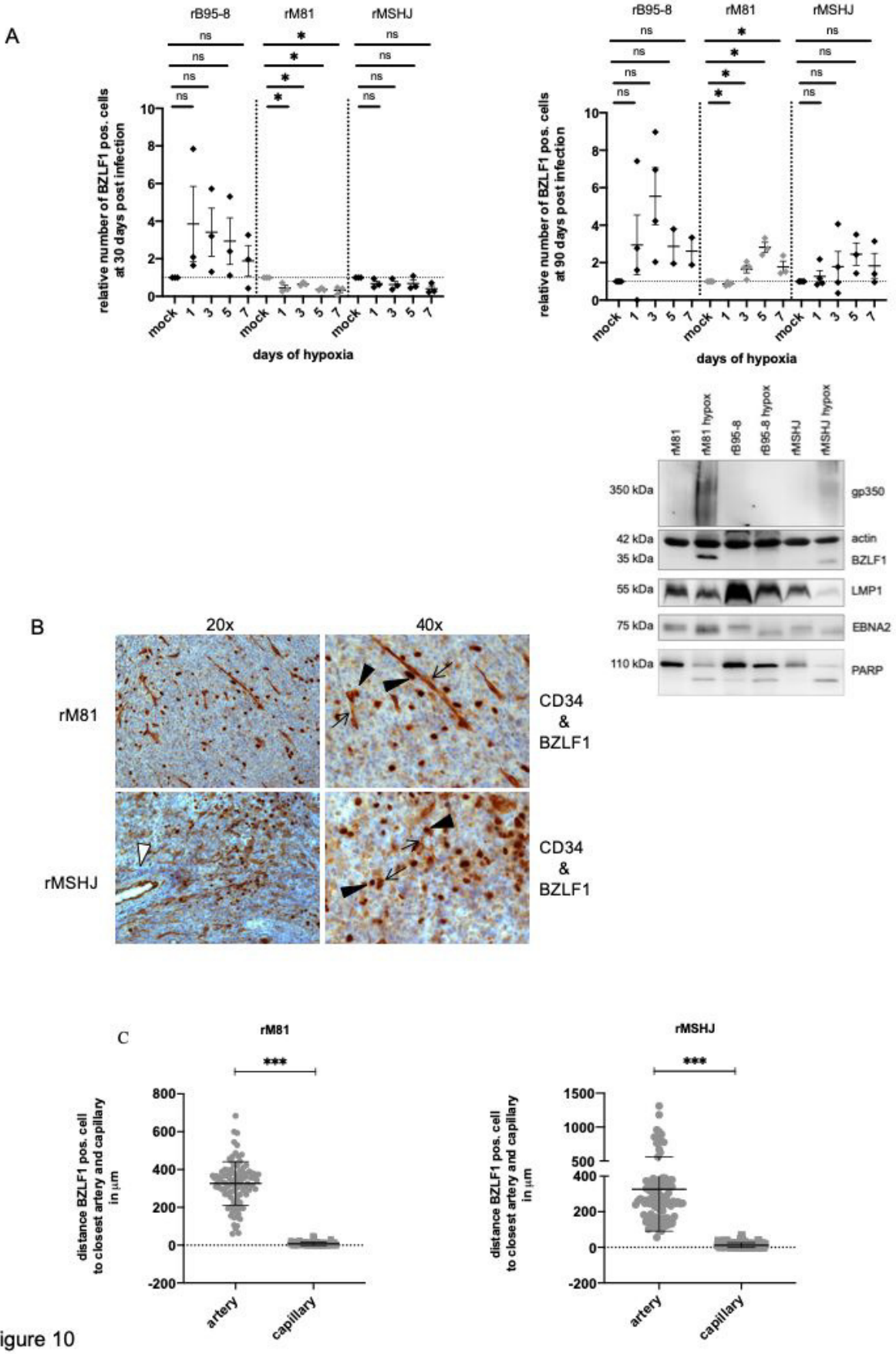

Figure 10